

Pressure and temperature dependence of the $C_2H_3O + NO_2$ reaction

Katherine I. Barnhard, Alejandro Santiago, Min He, Federico Asmar and Brad R. Weiner¹

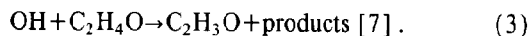
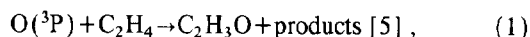
Department of Chemistry, University of Puerto Rico, Rio Piedras, PR 00931, USA

Received 17 December 1990

The temperature (295–374 K) and pressure (2.5–100 Torr) dependences for the rate constant of the $C_2H_3O + NO_2$ reaction have been measured by laser flash photolysis/laser-induced fluorescence kinetic spectroscopy. The temperature-dependent reaction for the decay of C_2H_3O in the presence of NO_2 is characterized over the measured region by the rate expression $k_{II} = (1.48 \pm 0.70) \times 10^{-11} \exp(80.7 \pm 23.4 \text{ K}/T) \text{ cm}^3 \text{ molecule}^{-1} \text{ s}^{-1}$. This rate expression is found to be independent of pressure. The results can be explained by a reaction mechanism involving the formation of an energized adduct which subsequently decomposes to products, most likely ketene and nitrous acid.

1. Introduction

Alkoxy radicals (RO) are important chemical intermediates in both combustion [1] and atmospheric [2] systems. The radicals can arise from a variety of hydrocarbon oxidation reactions, and can also be formed in various near-UV photolyses and photosensitized decompositions of ethers [3]. While a base of indirect kinetic data has been reported for chemical reactions of the simpler alkoxy radicals (e.g. methoxy, ethoxy) [4], no such information exists for the vinoxy radical. The vinoxy radical, C_2H_3O , is readily formed in the following oxidations of unsaturated hydrocarbons:



While alkoxy radicals have been shown to react slowly with trace atmospheric gases, such as hydrocarbons [8], they undergo fast reactions with NO_2 . Direct kinetic measurements of $RO + NO_2$ ($R = CH_3$, C_2H_5 , and $i-C_3H_7$) have been reported as a function of temperature and pressure [9]. In these studies, the association reaction to form $RONO_2$ is believed

to be the predominate pathway, but atom-transfer channels could not be ruled out. The reaction dynamics of the vinoxy radical provides an interesting case for study. Although technically an alkoxy radical, vinoxy more closely resembles an alkyl radical (formyl methyl), with the unpaired electron localized on the terminal carbon rather than on the oxygen atom of the molecule. Previous direct kinetic studies of the vinoxy radical with O_2 and NO have found pressure-dependent reactions with small, i.e. negligible, activation barriers [10]. In both cases, the primary product of the reaction was predicted to be a collisionally stabilized adduct with radical molecule addition occurring at the terminal carbon.

We report here a direct measurement of the temperature and pressure dependence of the gas-phase kinetics of the $C_2H_3O + NO_2$ reaction using a two-laser, pump-probe technique, laser flash photolysis/laser-induced fluorescence kinetic spectroscopy. In brief, the vinoxy radicals are produced by excimer-laser photolysis of methyl vinyl ether (MVE) at 193 nm, and are detected by laser-induced fluorescence (LIF) on the $B-\tilde{X}$ transition near 337 nm [11]. Bimolecular rate constants are obtained by monitoring the vinoxy radical disappearance as a function of NO_2 concentration in real time under pseudo-first-order conditions.

¹ To whom correspondence should be addressed.

2. Experimental

The experimental apparatus is shown schematically in fig. 1. C_2H_3O radicals are generated by the excimer-laser photolysis of methyl vinyl ether at 193 nm. The excimer laser used in these studies is a Lambda Physik LPX205i operating on the ArF transition (193 nm). Typical fluences for these studies were 50–75 mJ/cm². The time-dependent concentration of vinoxy radicals is monitored by LIF on the $B^2\bar{A}-X^2\bar{A}$ transition. Most of the experiments reported here were done by exciting the (100) transition at 337.0 nm, but several studies were also performed by using 342.1 nm excitation on the (001) transition. No discernible variations were observed in the rate-constant measurements for these different wavelengths. The probe-laser wavelengths were generated by a Lambda Physik 3002 tunable dye laser pumped by a Lambda Physik LPX205i excimer laser (pulsewidth \approx 20 ns) operating on the XeCl transition at 308 nm. All the LIF excitation wavelengths could be generated by using a single dye (*p*-terphenyl), and typically, pulse energies of 2–10 mJ/pulse were employed. The lasers are directed into a reaction chamber which consists of a 4-way stainless-steel cross (2.5 inch diameter) with 18 inch long brass extension arms along the laser propagation axis.

The extension arms each contain a conical light baffle and have UV-Suprasil windows mounted at Brewster's angle to reduce scattered laser light. Gas inlets are located along both arms, and the vacuum outlet is located on the stainless-steel cross. Gas pressures are measured at the exit of the reaction cell by a Baratron capacitance manometer. Metered flows of methyl vinyl ether, nitrogen dioxide and nitrogen (buffer gas) are mixed prior to entering the reaction zone, and are passed through the cell at total flow rates of 0.1–1.0 l/min. Methyl vinyl ether and NO_2 are prepared as 1:100 and 5:1000 mixtures, respectively, in buffer gas. Partial pressures of the reactants were calculated from measured flow rates and the total pressure. Typical reactant partial pressures were 0.3–1.0 mTorr MVE, 0–80 mTorr NO_2 , and 2.5–100 Torr N_2 buffer gas. Temperature-dependent studies were accomplished by wrapping the entire reaction vessel in heating tape, and monitoring the temperature in three different locations with a thermocouple. Temperatures were constant to within \pm 2 K.

The induced fluorescence is viewed by a high-gain photomultiplier tube (Hamamatsu R943-02) through a bandpass filter (Andover Corp, λ_{max} = 400 nm, fwhm = 60 nm), and a longpass filter (Schott WG360). The output of the photomultiplier tube is processed and averaged by a Stanford Research Sys-

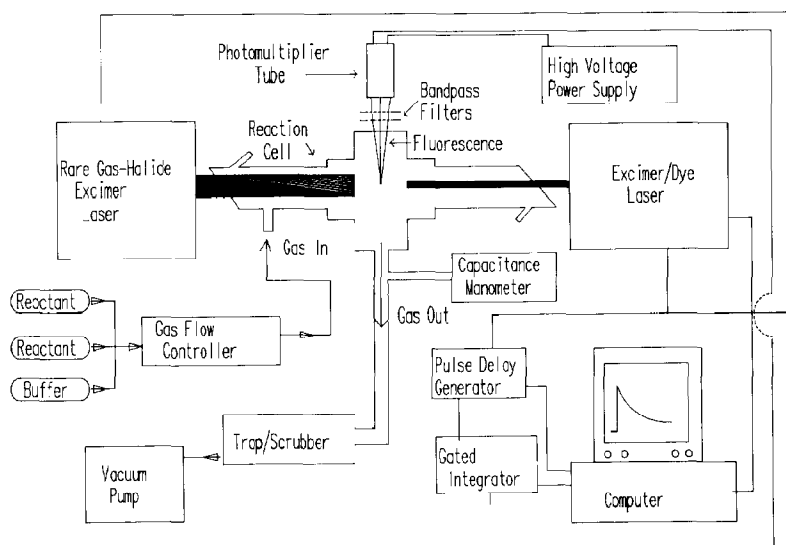


Fig. 1. A schematic diagram of the laser flash photolysis/laser-induced fluorescence kinetic spectroscopy apparatus.

tems gated integrator (model SR250), and then digitized and sent to a computer (Northgate 286) for display, storage, and analysis. Temporal profiles of the vinyoxy radical were recorded by scanning the delay time in between the two lasers with a digital delay pulse generator (Stanford Research Systems, model DG535). Data were typically collected at 30 Hz, and 10 laser shots were averaged for each temporal point. LIF excitation spectra were taken in a similar manner. At a fixed delay time between photolysis and probe lasers, the frequency of the dye laser was scanned while collecting the total fluorescence signal at the photomultiplier tube. The signal was processed, digitized and stored in the same manner as described above.

Experiments were conducted to measure the stable photoproducts following the 193 nm irradiation of MVE/NO₂ mixtures (1:10). These experiments were performed by placing these mixtures (total pressure = 50 Torr) in a 10 cm long infrared cell fitted with CaF₂ windows and measuring the FT-IR (Nicolet 740) spectrum prior to and after the 193 nm laser irradiation. UV irradiation times were varied from 1000–20000 laser shots.

The gases were purchased from the following suppliers and used without further purification: methyl vinyl ether (Matheson, 99%), nitrogen dioxide (Matheson, 99.5%) and N₂ (General Gases, 99.99%).

3. Results

Prior to beginning the kinetics experiments, we verified the production of the vinyoxy radical following 193 nm photolysis of methyl vinyl ether by recording the LIF excitation spectra from 335–350 nm. Our result agrees with the excitation spectrum reported in ref. [11]. From this spectrum, we chose the most intense bands at 337.0 (100) and 342.1 (001) nm to use for our kinetic studies. A typical kinetic decay of the vinyoxy radical in the presence of NO₂ is shown in fig. 2a. In the absence of reactant gas, the rate of disappearance of C₂H₃O is consistent with the diffusion of the radical out of the probe-laser beam. No difference was observed in the kinetic decay data measured by using other spectroscopic probe lines.

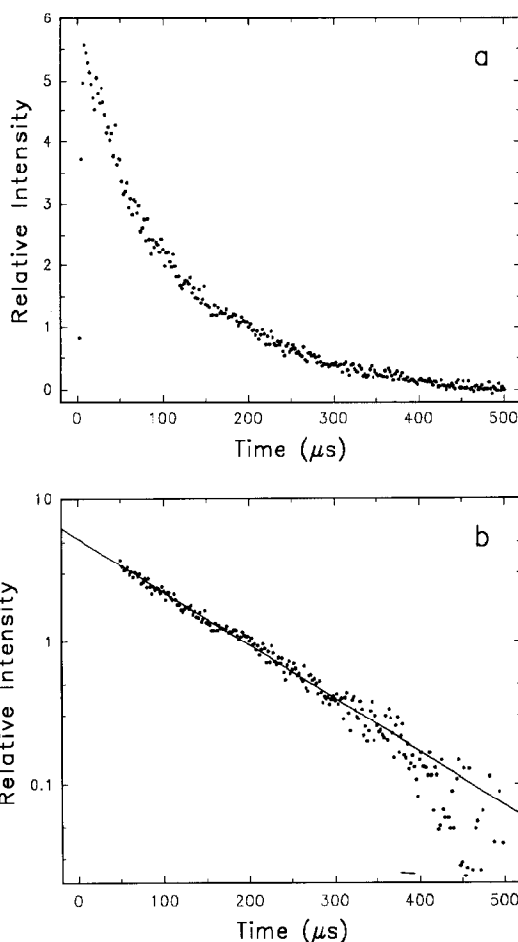


Fig. 2. (a) A typical temporal profile obtained under the following conditions: $P_{\text{MVE}}=0.0036$, $P_{\text{NO}_2}=0.0055$, $P_{\text{total}}(\text{balance N}_2)=10.06$ Torr, and $T=308$ K. (b) The logarithm of the relative intensity versus time of decay profile shown in (a). The line is a linear least-squares fit to the data.

In order to obtain second-order rate constants, k_{11} , for the C₂H₃O+NO₂ reaction, the pseudo-first-order rate constants, obtained from a linear least-squares fit to the slope of the logarithm of the decay (see fig. 2b), are plotted as a function of NO₂ pressure. Linear fits to the logarithmic decays were taken over 3–4 reaction lifetimes beginning at a delay time corresponding to at least 3000 gas kinetic collisions. This is to ensure that the vinyoxy radical, which is initially prepared with significant internal energy from the UV photolysis, is allowed to reach thermal equilibrium. A typical plot of the pseudo-first-order rate

constant, k' , versus the partial pressure of nitrogen dioxide, P_{NO_2} , is shown in fig. 3. The slope of this linear plot yields the bimolecular rate constant. We have measured the dependence of temperature and total pressure on this bimolecular rate constant. The results are summarized in table 1.

The temperature dependence of a bimolecular rate constant can be considered in terms of the Arrhenius equation, $k_{\text{II}} = A \exp(-E_a/RT)$, where A is the preexponential factor, E_a is the activation energy for the reaction, and R is the gas constant. Fig. 4 shows the dependence of k_{II} versus $1/T$. The linear least-squares fit to this line indicates a negative dependence, i.e. the reaction gets slower with increasing temperature for this reaction. The temperature-dependent rate constant for the reaction between 295 and 374 K can be expressed as $k_{\text{II}} = (1.48 \pm 0.70) \times 10^{-11} \exp(80.7 \pm 23.4 \text{ K}/T) \text{ cm}^3 \text{ molecule}^{-1} \text{ s}^{-1}$.

Table 1 shows the dependence of k_{II} on the total pressure in the reaction cell. Over the range of pressures measured, 2.5–100 Torr total pressure, we conclude that there is no discernible trend in the data, i.e. there is no pressure dependence.

FT-IR spectra of the photolysis mixtures were obtained. The major difference between the spectrum of the unphotolyzed and photolyzed mixtures is the growth of a band centered near 2350 cm^{-1} , which is

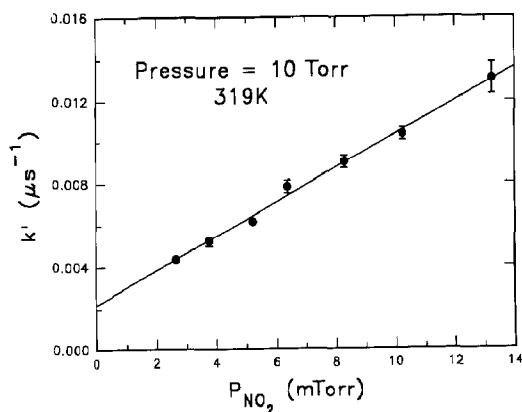


Fig. 3. A plot of the pseudo-first-order rate constants obtained (see fig. 2b) versus the partial pressure of NO_2 at a total pressure of 10 Torr and a temperature of 319 K. The error bars represent 2σ deviations. The line is a linear least-squares fit to the data, and the slope gives the bimolecular rate constant, k_{II} , at the given total pressure.

Table 1

The bimolecular rate constant, k_{II} , as a function of temperature and total pressure. The reported errors are 2σ

| | Temperature (K) | k_{II} ($10^{-11} \text{ cm}^3 \text{ s}^{-1}$) |
|--------------------------------------|-----------------------|------------------------------------------------------------|
| $P_{\text{total}} = 10 \text{ Torr}$ | 295 | 2.74 ± 0.32 |
| | 308 | 2.72 ± 0.21 |
| | 319 | 2.70 ± 0.17 |
| | 328 | 2.68 ± 0.24 |
| | 340 | 2.59 ± 0.23 |
| | 358 | 2.52 ± 0.17 |
| | 374 | 2.40 ± 0.14 |
| | Total pressure (Torr) | k_{II} ($10^{-11} \text{ cm}^3 \text{ s}^{-1}$) |
| $T = 295 \text{ K}$ | 2.5 | 1.92 ± 0.18 |
| | 3 | 2.41 ± 0.08 |
| | 5 | 2.98 ± 0.22 |
| | 15 | 2.75 ± 0.18 |
| | 30 | 2.53 ± 0.14 |
| | 50 | 2.46 ± 0.10 |
| | 70 | 2.44 ± 0.20 |
| | 100 | 2.74 ± 0.14 |

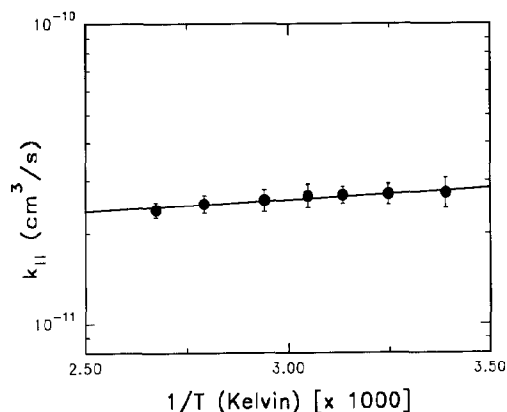
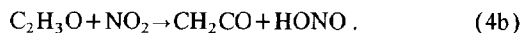


Fig. 4. A semi-logarithmic plot of the bimolecular rate constants, k_{II} , obtained at a total pressure of 10 Torr as a function of $1/T$ (K). The line is a linear least-squares fit to the data points, where the error bars are 2σ . See text for further explanation.

characteristic of CO_2 . The 2350 cm^{-1} band grows in as a function of irradiation time. While some changes in the C-H stretching region near 3000 cm^{-1} occur upon photolysis, no definitive assignments could be made to resolve the products.

4. Discussion

Consistent with previous kinetic work on the vinoxy radical [10], two reaction pathways can be postulated,

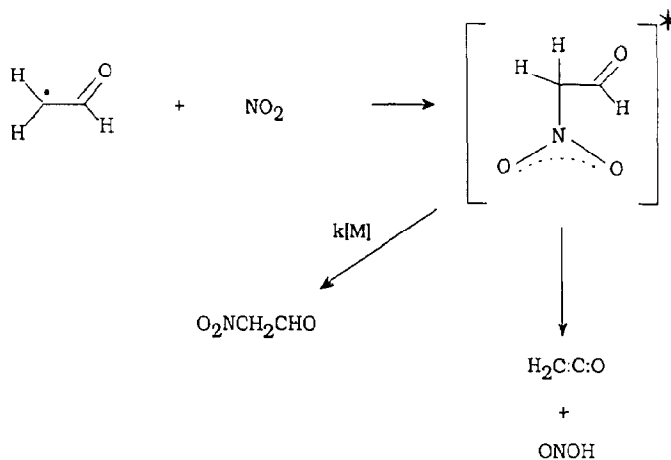


The first pathway, (4a), leads to the production of a pressure-dependent, stabilized addition product, nitroacetaldehyde ($\Delta H_{\text{RXN}4a} = -58$ kcal/mol), while the second process, (4b), corresponds to an H-atom transfer pathway ($\Delta H_{\text{RXN}4b} = -44$ kcal/mol)^{#1}. Reaction (4b) can proceed either by a direct abstraction mechanism, or by formation of an energized adduct, which can subsequently rearrange and decompose. For the case of either pathway, we assume that if an adduct is formed, addition of NO_2 occurs at the carbon position, because in its ground-state configuration, vinoxy is predicted to be more like a formylmethyl ($\cdot\text{CH}_2\text{-CH=O}$) radical than an ethenyloxy ($\text{CH}_2=\text{CH-O}\cdot$) radical [13]. The slightly negative temperature dependence of this reaction is indicative of a negligible activation barrier for the reaction. The result is consistent with previous findings on the temperature-dependent reac-

^{#1} Thermochemical values are either taken directly from the tables, or estimated by group additivity methods [12].

tions of vinoxy with O_2 and NO [10], and is often observed in radical-radical reactions [14]. These effects have been explained previously by having the reaction proceed through a bound complex separated from the final products by a small potential barrier. Depending on the magnitude of this potential barrier, the observed reaction rate can vary with respect to the "capture ratio" [15]. If the barrier from the bound state to the products is small enough, and the initial reactants are sufficiently energized, the reaction can be observed to have a negative temperature dependence. A similar type of mechanism, as shown in scheme 1, can be envisioned here. Nitrogen dioxide adds on the carbon-centered radical of the ground-state vinoxy molecule. The fate of this energized adduct, when it encounters the potential surface at the transition state between the reactants and the products, has at least two possible deactivation pathways (see scheme 1). These two routes are also consistent with the previously shown vinoxy radical pathways, (4a) and (4b).

The two pathways can be differentiated by measuring the effects of total pressure on the reaction. The apparent lack of a pressure dependence for the $\text{C}_2\text{H}_3\text{O} + \text{NO}_2$ reaction indicates that the formation of a stabilized nitroacetaldehyde is unlikely. This result is further substantiated by the fact that this molecule has never been isolated (to the best of our knowledge). It must be noted, however, that it is possible that for a system of this molecular size, which



Scheme 1.

can form an intermediate complex with many internal degrees of freedom, the high-pressure limit may already have been reached at 2.5 Torr total pressure [15].

Since the formation of a stabilized adduct is unlikely, the mechanism for the reaction is best explained by the decomposition of the energized adduct, e.g. pathway (4b) which can be pressure independent. The formation of ketene and nitrous acid is one possible scenario. Our attempts to find ketene by its well-known carbonyl stretching frequency ($\nu \approx 2100 \text{ cm}^{-1}$) [16] were unsuccessful. However, this may be due to secondary photolysis of the ketene at 193 nm [17], thermal decomposition of the energized products, or the rapid reaction of the ketene with initial reactants. Since we observe the production of CO_2 in our reaction cell, the oxidation of ketene by the excess NO_2 in the cell seems likely [18].

5. Conclusions

The fast reaction of vinoxy radical + NO_2 has been found to have (1) no appreciable barrier to reaction, and (2) no apparent pressure dependence over the range of 2.5–100 Torr. Our measurements lead us to conclude that the molecule proceeds through an energized collision complex to give $\text{C}_2\text{H}_2\text{O}$ and HONO. While the final products are the same as other alkoxy- NO_2 reactions, the mechanism appears to differ. In order to verify this definitely, more detailed experiments remain to be done. For example, a quantitative analysis, including branching ratios, of the final products of this reaction needs to be characterized.

The reaction has important consequences with respect to atmospheric chemistry. Due to the fast rate of this reaction at almost all conditions, we believe that this rate should be considered by kinetic modellers.

Acknowledgement

The experiments were performed in the Puerto Rico Laser and Spectroscopy Facility, which is co-sponsored by NSF-EPSCoR (Grant No. R11-

8610677) and NIH-RCMI (Grant No. RR-03541). We would also like to acknowledge kindly the partial support of the Air Office of Scientific Research (Contract No. F49620-89-C0070).

References

- [1] R.R. Baldwin and R.W. Walker, Symp. (Intern.) Combustion Proc. 18 (1981) 819.
- [2] B.J. Finlayson-Pitts and J.N. Pitts Jr., Atmospheric chemistry: fundamentals and experimental techniques (Wiley, New York, 1986) pp. 425–431.
- [3] K.O. McFadden and C.L. Currie, J. Chem. Phys. 58 (1973) 1213.
- [4] G. Baker and R. Shaw, J. Chem. Soc. (1965) 6965; H.A. Wiebe, A. Villa, T.M. Hellman and J. Heicklan, J. Am. Chem. Soc. 95 (1973) 7; J.R. Barker, S.W. Benson and D.M. Golden, Intern. J. Chem. Kinetics 9 (1977) 31; L. Batt and G.N. Robinson, Intern. J. Chem. Kinetics 9 (1979) 1045; R.A. Cox, R.G. Derwent, S.V. Kearney, L. Batt and K.G. Patrick, J. Photochem. 13 (1980) 149.
- [5] R.J. Buss, R.J. Baseman, G. He and Y.T. Lee, J. Photochem. 17 (1981) 389; K. Kleinermanns and A.C. Lutz, J. Phys. Chem. 85 (1981) 1966; H.E. Hunziker, H. Knepe and H.R. Wendt, J. Photochem. 17 (1981) 377; Y. Endo, S. Tsuchiya, C. Yamada, E. Hirota and S. Koda, J. Chem. Phys. 85 (1986) 4446; A.M. Schmoltner, P.M. Chu, R.J. Brudzynski and Y.T. Lee, J. Chem. Phys. 91 (1989) 6926.
- [6] V. Schmidt, G.Y. Zhu, K.H. Becker and E.H. Fink, 3rd European Symposium on Physico-Chemical Behavior of Atmospheric Pollutants, Ispra, Varese (1984).
- [7] K. Lorenz and R. Zellner, Ber. Bunsenges. Physik. Chem. 88 (1984) 1228.
- [8] L. Batt and G.N. Rattray, Intern. J. Chem. Kinetics 9 (1977) 549.
- [9] M.J. Frost and I.W.M. Smith, J. Chem. Soc. Faraday Trans. 86 (1990) 1751; R.J. Balla, H.H. Nelson and J.R. McDonald, Chem. Phys. 99 (1985) 323.
- [10] D. Gutman and H.H. Nelson, J. Phys. Chem. 87 (1983) 3902; K. Lorenz, D. Rhäsa, R. Zellner and B. Fritz, Ber. Bunsenges. Physik. Chem. 89 (1985) 341.
- [11] G. Inoue and H. Akimoto, J. Chem. Phys. 74 (1981) 425.
- [12] S.W. Benson, Thermochemical kinetics (Wiley-Interscience, New York, 1976).
- [13] M. Dupuis, J.J. Wedolski and W.A. Lester, J. Chem. Phys. 76 (1982) 488; E.S. Huyser, D. Felner, W.T. Borden and E.R. Davidson, J. Am. Chem. Soc. 104 (1982) 2956;

- M. Yamaguchi, T. Momose and T. Shida, *J. Chem. Phys.* 93 (1990) 4211.
- [14] R. Atkinson, D.L. Baulch, R.A. Cox, R.F. Hampson Jr., J.A. Kerr and J. Troe, *J. Phys. Chem. Ref. Data* 18 (1989) 881.
- [15] L.F. Phillips, *J. Phys. Chem.* 94 (1990) 7482.
- [16] W.F. Arendale and W.H. Fletcher, *J. Chem. Phys.* 26 (1957) 793.
- [17] D.J. Nesbitt, H. Petek, M.F. Foltz, S.V. Filseth, D.J. Bamford and C.B. Moore, *J. Chem. Phys.* 83 (1985) 223.
- [18] J.K. Crandall, S.A. Sojka and J.B. Kamin, *J. Org. Chem.* 39 (1974) 2172;
P. Michaud and C. Ouellet, *Can. J. Chem.* 49 (1971) 294, 303.